ADVANCED MATERIALS

DOI: 10.1002/adma.200800125

Millimeter-Scale Assembly of CdSe Nanorods into Smectic Superstructures by Solvent Drying Kinetics**

By *Claudia Querner, Michael D. Fischbein, Paul A. Heiney,* and *Marija Drndić**

Molecular and materials self-assembly are important fundamental principles and strategies for nanofabrication and nanotechnology in general.[1] Hierarchical organization of molecules, polymers, and particles can be induced by various interactions, such as hydrogen bonding and ionic interactions. Furthermore, capillary, electric, magnetic, and entropic forces can influence the assembly of solid-state materials over a range of length scales.[2]

Recently, colloidal nanocrystals have emerged as building blocks in nanotechnology research, particularly because of their unique size- and shape-dependent physical properties.[3] Significant progress in synthesis procedures has made it possible to prepare high-quality samples of controlled composition, size, and shape.[4] Owing to their favorable optical and electronic properties, semiconducting nanocrystals are used in many applications, including devices (e.g., light emitting diodes,[5] memory,[6] and solar cells[7]) and biomedical labeling.[8]

Large-scale ordered structures consisting of nanocrystals can have unique properties with broad-ranging applications, and many results on nanocrystal self-assembly have been reported. In the case of spherical nanocrystals large-area close-packed arrays in two and three dimensions have been produced[9,10] and binary-superlattices composed of two nanocrystal types have recently been demonstrated.[11]

Ordered self-assembly of anisotropic nanocrystals, such as nanorods (NRs), is more complicated than that of spheres because of their reduced shape symmetry, though significant progress has been made. Isotropic and nematic liquid-crystalline phases have been observed by birefringence imaging of CdSe NRs in solution after they have been allowed to phase-segregate over days.[12] In the solid state, CdSe NRs have been observed in side-to-side arrangements, forming micrometer-long NR tracks,[13] which can themselves be arranged with local order (up to ca. 5 NR tracks) when drop-cast from particular high-boiling nonsolvents.[14] Highly monodisperse CdS and compositionally asymmetric CdSe/CdS core–shell NRs synthesized by the seeded-growth approach have been recently found to form vertical superlattices of ca. 1 μm^2 area.[15,16] CdSe NRs can also assemble head-to-tail into network-type patterns,[17] a behavior which has been attributed to dipolar interactions. Ordering in $BaCrO_4$ NR systems has been induced by modifying the NR–surfactant–solvent interactions by processing NRs out from microemulsions and varying the water content in the mixture.[18] The addition of excess surfactant to concentrated solutions of Au NRs, together with slow drying, has also been shown to produce ordered assemblies at the micrometer scale.[19,20] Additionally, Langmuir–Blodgett techniques have been used to induce micrometer-scale ordering of Au, $BaCrO_4$, and $BaWO_4$ NRs.[21] Other surface interaction-based methods include vertical assembly of aligned CdS NRs on highly oriented pyrolytic graphite across ca. 2 μm^2.[22] An external electric field applied during the solvent evaporation of a NR-containing solution has been effective at enhancing the extent of alignment for Cd-based NRs on carbon grids[23] and across electrode gaps inside devices.[15,24]

In addition to the assembly mechanisms mentioned above, fluid flow in a drying droplet can itself be an important factor in guiding assembly. It is well known that a pinned edge of a drying droplet leads to capillary flow of material from within the droplet volume to the pinning site (usually the entire perimeter of the droplet).[25,26] This behavior results in a so-called coffee-ring region and has been demonstrated for many materials and at a range of size scales.[27–31] However, most cases have involved micrometer-scale and larger particles. In the nanometer-scale regime, examples of capillary-flow-mediated assembly include disordered Ag nanoparticle arrays,[32] aligned nanotubes[33,34] and diblock copolymers,[35] and zigzag DNA assemblies.[36]

We report here the use of capillary flow in a drying droplet of solution, containing highly monodisperse CdSe NRs, to rapidly form CdSe NR smectic superstructures. Importantly, this approach to assembly does not require any particular synthesis or solvent, pretreatment of the substrate or NRs, or external electric fields, and is achieved rapidly under nonequilibrium conditions. These superstructures are formed as capillary flow causes many NR tracks, which act as building blocks, to the

[*] Dr. C. Querner, M. D. Fischbein, Prof. P. A. Heiney, Prof. M. Drndić
Department of Physics and Astronomy
University of Pennsylvania
Philadelphia, PA 19104 (USA)
E-mail: drndic@physics.upenn.edu

[**] This work has been supported by an Alfred P. Sloan Fellowship, NSF (NSF Career Award DMR-0449533, NSF NSEC DMR-0425780, MRSEC DMR05-20020) and ONR (YIP N000140410489 and N000140510393). M.F. acknowledges funding from the NSF-IGERT program (Grant DGE-0221664). The authors also appreciate fruitful discussions with Prof. Tom Lubensky during the preparation of the manuscript. Finally, the authors thank Robin Havener for assisting with AFM imaging. Supporting Information is available online from Wiley InterScience or from the authors.

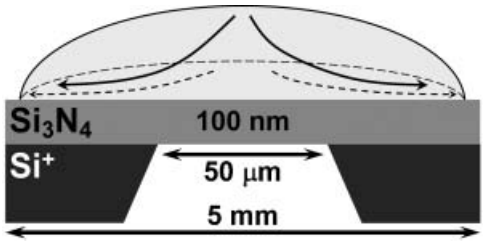

Scheme 1. Si_3N_4 membrane device onto which a droplet containing NRs has been deposited. Initially, the droplet wets the surface entirely. During the solvent evaporation it contracts and can become pinned on the substrate, leading to an outwards materials flow as indicated by the gray arrows.

perimeter of the droplet (Scheme 1). The NR tracks, which can be up to 30 μm in length and composed of up to thousands of single NRs oriented side-to-side, are formed independently at high local concentrations throughout the droplet. As the NR tracks arrive at the droplet perimeter, the capillary pressure directed radially outward from the droplet center tends to laterally stack the NR tracks concentrically. This process leads to a smectic superstructure that continues to grow inward from the droplet perimeter until no more material flows to the area, a result of possible factors including droplet de-pinning and complete solvent evaporation. The resulting smectic superstructure consists of parallel NR tracks, themselves aligned parallel to each other and to the coffee-ring contours, and therefore the individual NRs are aligned perpendicular to these contours. We have used this technique to achieve smectic superstructures up to the millimeter scale, which is considerably larger than previously reported CdSe NR assemblies.[13–16]

In addition to large smectic superstructures in the coffee ring, we have observed many smaller ordered NR assembly types near the ring (e.g., NR-track bundles and clusters). NRs can only move while in solution, and these smaller NR assemblies, while in transit to the ring, were made immobile by complete solvent evaporation and therefore offer insight into the intermediate stages of capillary-flow-mediated NR superstructure formation.

We study the structural details of the NR superstructures by transmission electron microscopy (TEM), atomic force microscopy (AFM), optical spectroscopy, and small angle X-ray diffraction (SAXS). Optical spectroscopy and SAXS showed no evidence of significant pre-formation of NR superstructures in solution, suggesting that the formation of the smectic superstructures indeed occurs due to the capillary-flow-mediated stacking of NR tracks initiated by droplet pinning on the substrate surface. Engineering pinning sites by patterning features or by other methods[37,38] may therefore offer further control of superstructure assembly over large areas.

Highly monodisperse 5 nm × 20 nm CdSe NRs were prepared using a modification of a procedure from the literature.[39] They exhibited a size distribution of <5% in diameter and <10% in length. The NRs were dispersed in hexane/octane solvent mixtures (ratio 9:1 by volume, unless otherwise stated) for further characterization (Supporting Information, Fig. S1). For direct comparison with previous studies, we note that the NRs used for this study had an aspect ratio of ca. 4, and are shorter than what is commonly seen in the existing literature on NR self-assembly where, for example, NRs had aspect ratios of ca. 6–7 for CdSe,[13,14] ca. 13–18 for gold,[20] and even up to 150 for $BaWO_4$.[21]

Samples were prepared by drop-casting ca. 5 μL of NR solution without any prior treatment of the substrate, resulting in a droplet with initial diameter of ca. 5 mm, and allowing the solvent to evaporate at room temperature in air. Some samples were then put under vacuum for additional drying, though this did not lead to any noticeable differences in the final superstructures. We used thin suspended Si_3N_4 membranes as substrates because they allow for characterization by TEM (JEOL 2010F) and AFM (Veeco EnviroScope) while providing a smooth and uniform surface.

Figure 1 shows TEM images of NR smectic superstructures at a range of magnifications. The smectic superstructures are composed of many NR tracks (a lamella) with length up to 30 μm. The macroscopic coffee-ring area of the substrate over which this smectic superstructure assembly occurred was ca. 0.2 mm^2 (the perimeter of the ring ca. 6 mm and its width ca. 30 μm). The NR tracks shown are the basic assembly blocks that align parallel to the coffee-ring contours while the individual NRs, within these tracks, are aligned perpendicularly. This is in contrast to DNA[36] and carbon nanotubes,[33,34] where these long, individual molecules align parallel to the coffee-ring contours. The NR-track smectic superstructures are stable and TEM images show no changes even after annealing at ca. 100 °C.

Figure 1 shows that, in contrast to a perfect liquid-crystalline phase, there are discontinuities and void regions in the NR assembly. Qualitatively similar lamella-like superstructures with voids have been reported for other systems, for example, the fd-virus/poly(*N*-isopropylacrylamide) system,[40] in which case the voids were isotropic regions of the polymer matrix expelled from the lamellae made of the rod-like virus, a segregation favored by entropic forces. In our system, no such additional matrix material was present and the voids are empty, as confirmed by AFM height analysis (Fig. 2 and Supporting Information, Fig. S2). The observed smectic superstructure irregularities are energetically costly and suggest that intratrack interactions are stronger than intertrack interactions; NR tracks favor remaining intact as opposed to partially disassembling and contributing some NRs to fill local smectic superstructure discontinuities. Additionally, NR tracks can bend without breaking, which further suggests that entropic forces are not the sole assembly mechanism. The degree of NR-track bending observed in individual tracks can be quite dramatic. Figures 1g,h show examples of many NR tracks with bends exhibiting small radii of curvature while still maintaining a high degree of concentricity. NR tracks are seen to bend up to 60° away from their long axis, occurring over as

ADVANCED MATERIALS

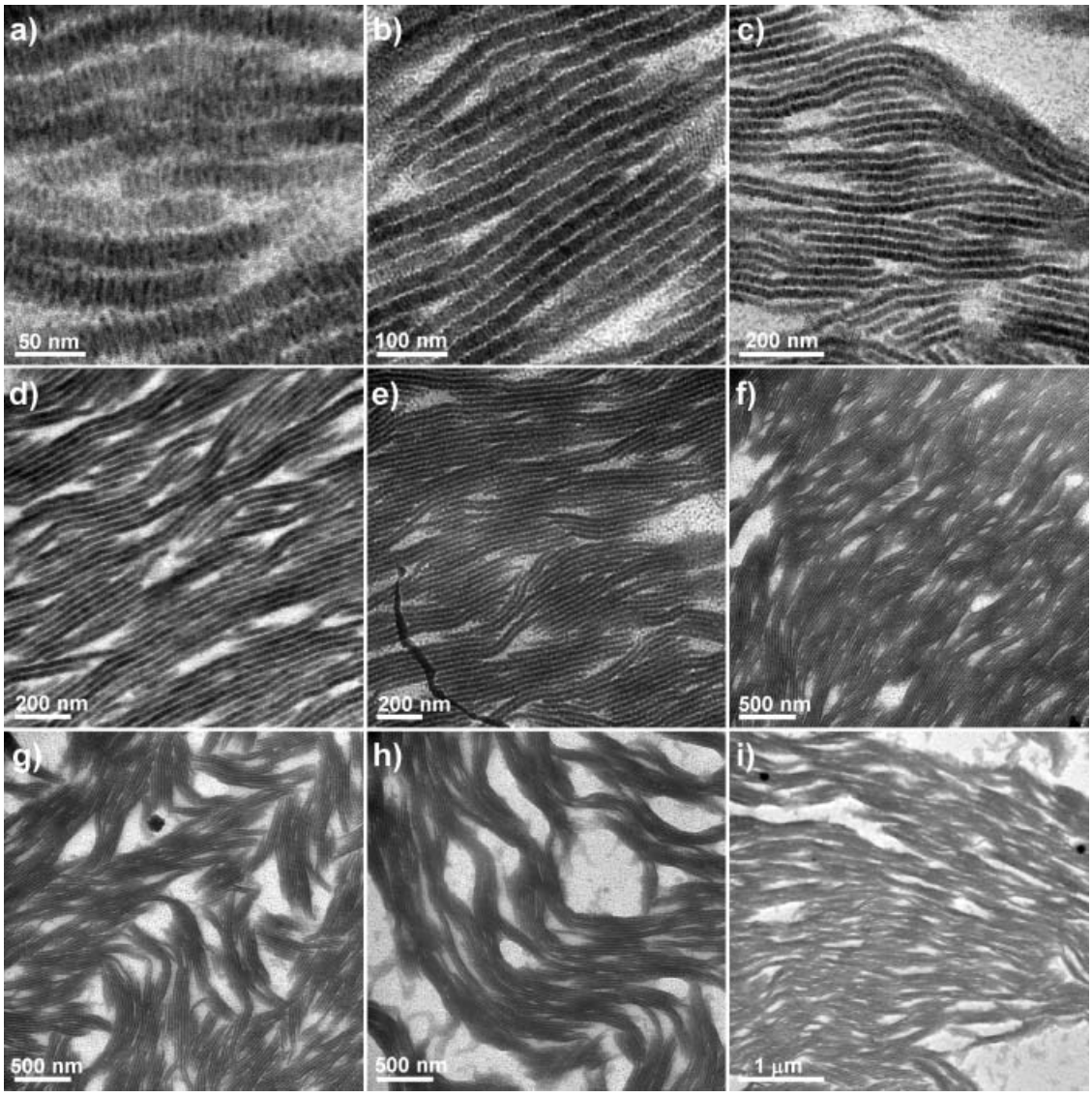

Figure 1. TEM images of CdSe NR tracks assembled into extended lamella-like superstructures shown at various magnifications. NRs are organized side-to-side into long tracks (up to several tens of micrometers). These tracks stack roughly parallel to each other into a smectic superstructure. The overall unidirectional orientation of the lamellae was parallel to the coffee-stain outline. The initial NR concentration was 5×10^{-7} mol · L^{-1}. NR tracks can also exhibit strong bending (g,h). More zoom-in TEM images of some of these bends can be found in the Supporting Information (Fig. S3).

little as ca. 100–150 nm track length (see also Supporting Information, Fig. S3). This degree of bending is most frequently observed for isolated regions of the smectic superstructure, found adjacent to the coffee ring.

While in transit to the droplet perimeter, NR tracks can also form interesting structures, which often come to rest near the coffee ring, before they are assimilated into the full smectic superstructure (see Figs. 1g,h). Figures 3a,b show many clusters, each containing ca. 10 NR tracks, closely packed together and, overall, oriented isotropically with respect to each other. The tracks within these clusters are all of similar length (ca. 200–500 nm). These clusters were observed along the entire inner perimeter of one particular coffee ring of radius ca. 1 mm and width ca. 3–5 μm. Though this specific cluster assembly was not always present in the coffee rings, we frequently observed the coffee rings to be composed of concentric ''bands'' of pattern types. The coffee rings are usually composed of a dense middle band flanked by bands of lower NR-track concentration (see Supporting Information, Figs. S4 and S5). Often the dense middle band is continuous, with a high degree of track–track ordering (Fig. 1). The flanking bands are discontinuous (Figs. 1g,h) and have a reduced track–track ordering (Fig. 3a). In these regions, smaller NR-track structures can form, which tend to group into NR-track clusters.

Examples showing the transition between concentric band regions can be seen in the AFM image in Figure 2 and in the Supporting Information, Figures S4 and S5. This behavior

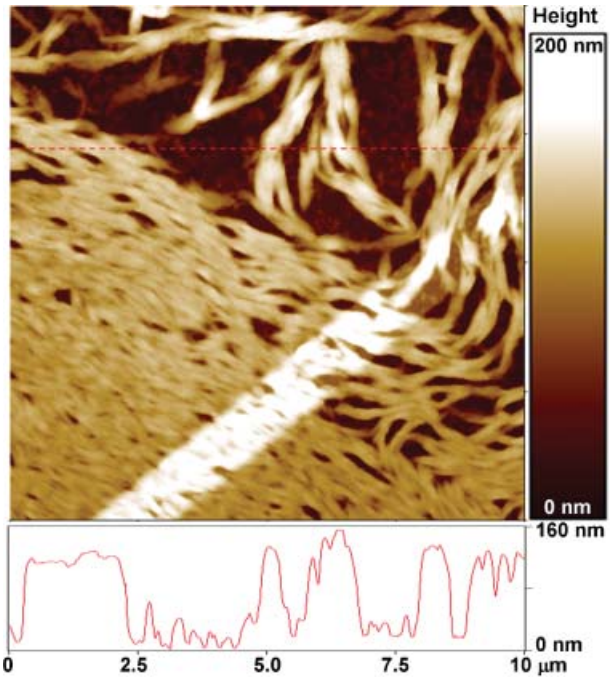

Figure 2. 10 μm × 10 μm AFM image of CdSe NR superstructures with its corresponding height analysis along the red dashed line. The bright, diagonal structure in the lower right corner is a gold wire pattern on the Si_3N_4 substrate. More zoom-out AFM images can be found in the Supporting Information (Fig. S2). The particular region in this image shows the transition between the dense assembly of tracks into lamellae and a sparser region containing bent structures, consisting of up to ca. 10 tracks in parallel.

suggests that, during evaporation, solvent can accumulate in disconnected regions on the substrate,[41] thereby constraining the extent of smectic superstructure formation of the NRs contained in these regions.

Capillary solvent flow is known to carry a significant portion, or in many cases all, of the material contained in a drying droplet to the coffee ring.[25–31] We observed in all experiments that a significant number of NRs occupy the regions between the coffee ring and the center of the droplet. Though the extent of smectic superstructure formation is reduced in these regions, we do observe a variety of revealing assembly trends. We varied the concentration of the NR-containing droplets over two orders of magnitude (5×10^{-8} to 5×10^{-6} mol · L^{-1}) as well as the evaporation rate to probe their influence on the NR assembly dynamics in these non-coffee-ring regions.

Low concentration (5×10^{-8} to 1×10^{-7} mol · L^{-1}) corresponds to the range of sub-monolayer to monolayer surface coverage. The TEM images show, as expected, a rather isotropic, randomly ordered array of NRs (Supporting Information, Fig. S6). The overall order parameter is close to zero ($S = 0.08$); a few rods align parallel to each other, but usually no more than ca. 5–10. On increasing the ratio of high-boiling solvent in the solvent mixture, using a 1:1 hexane/octane mixture instead of the 9:1 ratio, and therefore slowing down the evaporation, we do see some longer tracks of up to ca. 20 rods, but overall there is no significant increase in the order. This is also true when drop-casting from a pure octane solution.

On increasing the concentration to ca. 2×10^{-7} to 5×10^{-7} mol · L^{-1} we started to observe the presence of short NR tracks. The average length of these NR tracks is ca. 100–150 nm, corresponding to ca. 15–20 NRs. These NR tracks are arranged randomly with respect to each other, forming an isotropic network structure (Figs. 3d–f). From the TEM images, the interrod spacing, which is ca. 1.2–1.5 nm within monolayers, seems to be reduced. However, statistical analysis of the inter-NR spacing revealed no significant decrease. The apparent higher density within the tracks can be explained by the presence of a second layer of NRs stacked onto the first in a zigzag-like vertical structure. Figure 3d shows examples of additional NRs filling in the interstitial sites of a single NR track. Within the first layer the NR–NR spacing is ca. 1.2 nm due to the ligands, with the next layer offset with respect to the first one by roughly the radius of one NR plus the length of the ligand. That is, the three-dimensional (3D) smectic superstructures are likely several stacked planes of 2D smectic superstructures, each layer offset from those it touches, that is, ABAB-type vertical assembly. Furthermore, AFM analysis revealed that these superstructures are thick, ca. 100–150 nm, which is much larger than the diameter of a NR with ligand (Figs. 2 and S2).

At higher concentration (1×10^{-6} to 5×10^{-6} mol · L^{-1}) NRs assemble into the patterns seen in Figure 3c. The NR tracks are longer (hundreds of nanometers up to ca. 1 μm and containing hundreds of NRs) and NR tracks bundle together. The number of tracks in a bundle is typically fewer than ten and the bundles are arranged randomly with respect to each other. Furthermore, the NR tracks are not all lying in the same plane; some are on top of others, crisscrossed. This kind of pattern is always observed homogeneously across the entire substrate (ca. 5 mm × 5 mm), without qualitative variation (see Supporting Information, Fig. S8).

Though the non-coffee-ring regions are densely populated with NR tracks, we do not observe smectic superstructures in these regions. The bundles in Figure 3c are the most extensively ordered structures observed outside of the coffee ring. These observations indicate that smectic superstructure assembly requires both the presence of NR tracks and capillary flow to a pinning site.

To further characterize the origin of CdSe NR smectic superstructure assembly, we checked for the presence of NR ordering in solution. We performed SAXS and optical spectroscopic measurements on samples at different concentrations. CdSe NRs were characterized in solution by absorption spectroscopy (USB2000 spectrometer, Ocean Optics). Figure 4a shows absorption curves obtained for an initial, freshly prepared solution (black line), that has been concentrated (by a factor of 10) by slow solvent evaporation (black circles) and allowed to stand undisturbed for 10 days (gray circles). Normalization of these curves to a comparable absorbance at the excitonic peak revealed no significant

ADVANCED MATERIALS

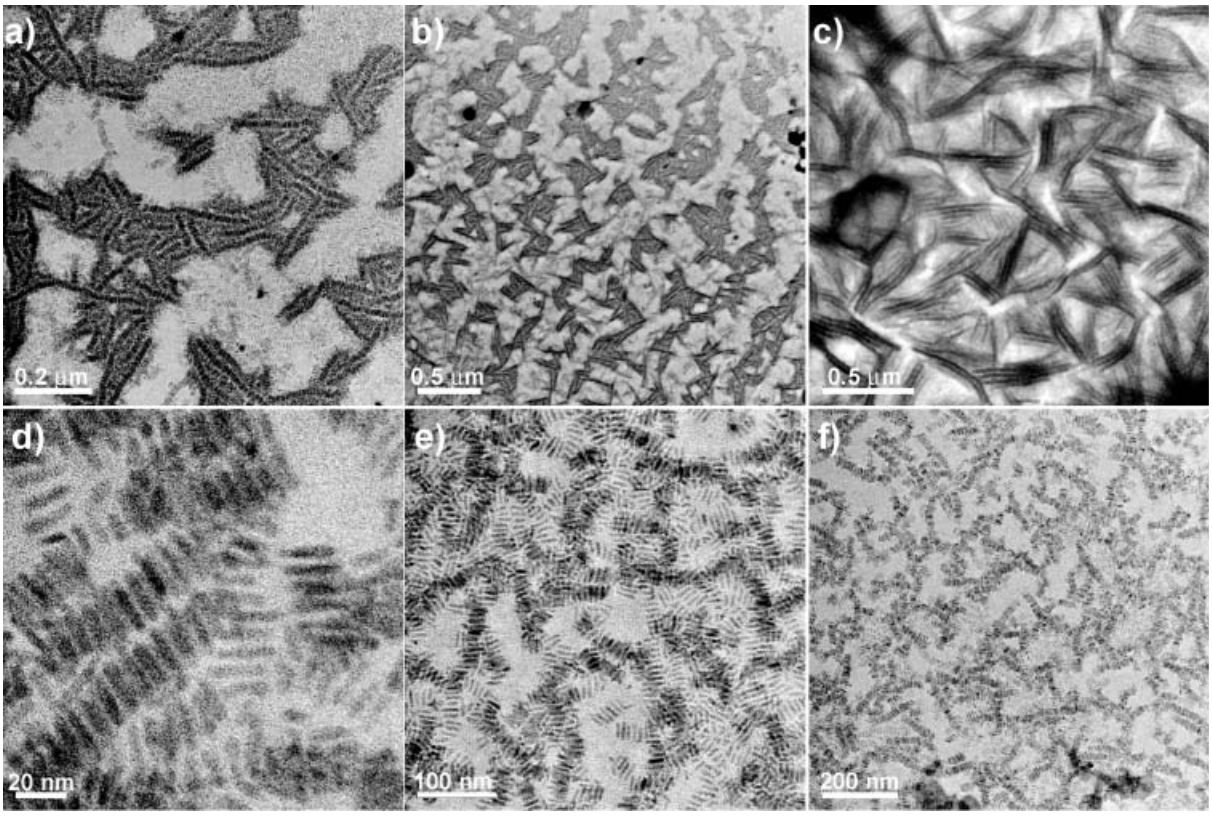

Figure 3. a,b) TEM images, with different magnifications, of assembly patterns in the inner perimeter of the so-called coffee-stain ring, formed by CdSe NRs drop-cast from medium-concentration solutions (5×10^{-7} mol · L^{-1}). We observed the formation of medium-size tracks (several hundred nanometers) packing randomly into clusters. These clusters extended along the whole ring (radius ca. 1 mm, width ca. 5 μm). c) TEM image of superstructures formed by CdSe NRs drop-cast from concentrated solutions (5×10^{-6} mol · L^{-1}). We observed the formation of medium-size tracks (several hundred nanaometers up to ca. 1 μm) packing side-by-side into bundles of ca. 5–10 tracks. These bundles then pack relatively closely on the surface but with no apparent long-range order (see also Supporting Information, Fig. S8). d–f) TEM images of short CdSe NR tracks, containing tens of NRs, shown at various magnifications (see also Supporting Information, Fig. S7).

differences between the NR solutions up to ca. 5×10^{-6} mol · L^{-1}.

We carried out SAXS measurements for hexane/octane (9:1) solutions with NR concentrations of 4×10^{-8}, 9×10^{-7}, and 5×10^{-6} mol · L^{-1}, also used in our droplet-drying experiments. The highest concentration corresponds to 0.2 vol % or 1 wt %. Figure 4b shows the results of these measurements. Even in the highest concentration used in our study, no maxima were observed in the SAXS pattern, indicating the absence of significant preformed aggregates in the solution in this concentration regime. For reference, Jana et al. previously presented SAXS measurements on Au NRs forming small clusters (ca. 30 NRs) in solutions at 0.001 vol %,[20] (ca. 50 times more dilute than our most concentrated case). These SAXS and optical measurements suggest that even at concentrations of 5×10^{-6} mol · L^{-1}, NR tracks do not form in solution.

Assuming the case of a slow uniform solvent evaporation, the concentration of the remaining droplet increases continuously and, consequently, the free volume available for each NR decreases. The NRs start to aggregate by aligning side-by-side, partly due to attractive forces such as capillary and van der Waals.[17] In addition to these attractive forces between NRs, entropy also plays an important role. Smectic ordering of NRs leads to a maximum of excluded volume per NR. This gain in translational entropy overrides the loss of orientational entropy associated with particle alignment and, in the presence of these entropic forces only, a close-packed smectic liquid phase would be observed.[42,43] The aspect ratio of NRs used here is ca. 4. For a case of 3D entropy-driven assembly of hard spherocylindrical rods using entropy as the main assembly mechanism, Bolhuis and Frenkel predict that the smectic phase first becomes stable at aspect ratio 3.1,[44] which is consistent with our observations of smectic superstructures since the NR volume fraction at the final phases of solvent drying should be very high. However, in longer NRs in solutions with aspect ratios of ca. 20, Li et al. have found that liquid-crystalline phases in NR solutions form at lower concentrations than predicted by the hard spherocylindical rod model, indicating that attractive interaction between the NRs is important in the formation of liquid-crystalline phases.[45] Futhermore, Talapin et al. have suggested that

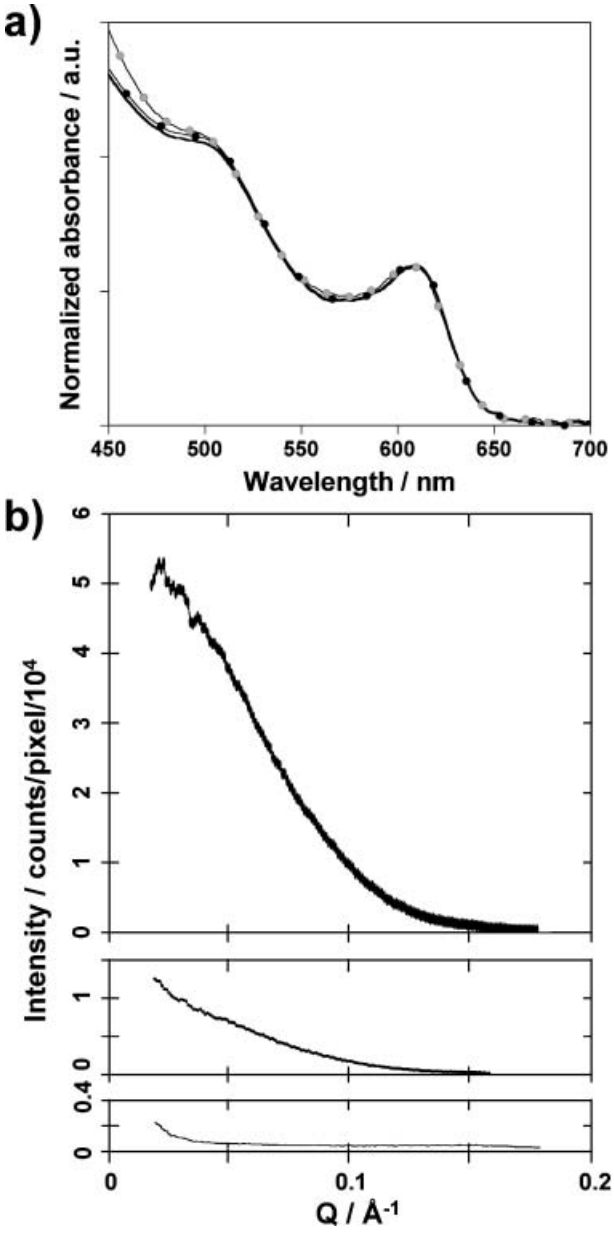

Figure 4. a) Absorption spectra of CdSe NRs recorded in hexane/octane (ratio 9:1 by volume). All spectra are normalized to the same absorbance at the excitonic peak. The black line represents the spectrum of a freshly prepared, medium-concentration solution, which was then concentrated by a factor of 10 by slow solvent evaporation over 5 days (black circles). This solution was finally allowed to stand undisturbed for 10 days (gray circles). There are slight variations at higher energies, that is, at wavelengths <500 nm, however, these changes seem not to be significant enough to indicate preformation of NR aggregates present in solution phase. b) SAXS results for CdSe NR solutions in hexane/octane at different concentrations: 4×10^{-8} (bottom), 9×10^{-7} (middle), and 5×10^{-6} mol $\cdot$ L^{-1} (top). $Q = 4\pi \sin\theta/\lambda$, where 2θ is the scattering angle and λ is the X-ray wavelength (1.5418 Å). The absolute intensity scales are the same in all three cases. The increase in intensity with increasing concentration clearly shows that the X-ray scattering is sensitive to the presence of NRs, but the lack of any observable peak at finite Q indicates that there is no detectable formation of preformed NR aggregates in solution.

the existence of isolated NR tracks, which we also observe, indicates that factors other than entropy, such as electrostatic forces between NRs, may govern NR assembly.[14] CdSe NRs have a large permanent dipole moment[46] and attractive dipolar interactions between adjacent NRs could lead to antiparallel side-by-side pairing of dipole moments[13] that could stabilize the smectic phase at lower concentrations.[47]

In addition to the equilibrium factors (entropy, capillary, and electrostatic forces), an important distinction in our case is that NR assembly occurs despite fast evaporation and is, in fact, *facilitated* by the inherently nonequilibrium outward solvent flow transporting the material to the perimeter.

The perimeter of a droplet is often pinned to the substrate. As the droplet dries the pinning results in fluid flow such that material throughout the droplet volume is transported radially outward and accumulates at the perimeter. The TEM images of isolated and highly bent NR tracks suggest that, once assembled into long NR-tracks, the individual NRs are no longer able to move freely and the NR tracks act as a single object that can only move as a whole. The formation of smectic superstructures is therefore a process of assembling entire NR tracks with one another, which is achieved by means of fluid flow during solvent evaporation. As NR tracks in the droplet flow to the perimeter their orientation may be random. However, as a consequence of the radial pressure caused by the fluid flow, the NR tracks are reoriented to be parallel to the perimeter once they arrive. As NR tracks continue to arrive at the perimeter, they pack laterally and begin to form superstructures. Additionally, the newly arriving NR tracks reinforce the concentric close-packing and provide structural integrity for the growing superstructure.

In conclusion, we have shown that rapid millimeter-scale assembly of CdSe NR smectic superstructures can be achieved by exploiting capillary flow of a pinned droplet. The flow orients many NR tracks, each formed individually, due to strong NR–NR interactions, parallel to each other and to the droplet edge, thereby forming a coffee ring. Scattering measurements indicate no preformation of NR tracks or smectic superstructures in solution at initial droplet concentrations, consistent with a capillary-flow assembly mechanism. Templating methods for engineering the pinning sites of a drying droplet may therefore allow patterning of more complicated NR smectic superstructures over large areas.

Experimental

Nanorod Synthesis: CdSe NRs were prepared using a standard hot injection method [39]. In detail, the Cd precursor was prepared by heating cadmium oxide (61.7 mg, Aldrich, 99%), decylphosphonic acid (227.3 mg, Alfa Aesar, 99%), and tri-*n*-octylphosphine oxide (2.998 g, Aldrich, 90%) at 300 °C under inert atmosphere. Then, selenium powder (74.1 mg, Aldrich, 99.99%) dissolved in tri-*n*-octylphosphine (2.00 g, Aldrich, 90%) was injected rapidly at 290 °C. After 15 min, the heat source was removed to stop the reaction. The NRs were precipitated and purified by washing several times with methanol.

ADVANCED MATERIALS

Finally, CdSe NRs were redispersed in hexane or hexane/octane mixtures for further characterization.

NRs were characterized in solution by absorption and emission spectroscopy using USB2000 and USB4000-FL (excitation: 518 nm LED, 35 μW) spectrometers, respectively, from Ocean Optics. TEM images were taken with a JEOL 2010F electron microscope, operating at 200 kV.

Sample Preparation: Solutions with NR concentrations between 4×10^{-8} and 5×10^{-6} mol · L^{-1} were prepared in hexane/octane solvent mixtures (ratio 9:1, unless otherwise stated). The substrate (ca. 5 mm × 5 mm) consists of p-doped silicon covered by a ca. 100 nm thin layer of Si_3N_4. Photolithography, followed by plasma and chemical etching, allows the controlled removal of a ca. 50 μm × 50 μm-wide region of the silicon, resulting in a suspended Si_3N_4 membrane window. Samples were prepared by drop-casting ca. 5 μL of the solution without any prior treatment of the substrate and allowing the solvent to evaporate at room temperature in air for ca. 1–2 h. The droplets consistently wet the entire substrate surface and were macroscopically dry within a few minutes. Additional waiting or application of vacuum was only for the purpose of complete drying and did not interfere with the formation of the assembly patterns.

Small Angle X-ray Scattering: SAXS measurements were performed using Cu $K\alpha_1$ radiation from a Bruker-Nonius FR-591 rotating anode X-ray source with a 0.2 mm × 0.2 mm filament operated at 3.4 kW. The beam was collimated and focused by a single bent mirror and sagittally focusing Si (111) monochromator, resulting in a 0.3 mm × 0.4 mm spot on a Bruker-AXS Hi-Star multiwire area detector. An integral vacuum was maintained along the length of the flight tube and within the sample chamber. The capillaries (diameter 1.0 mm, Charles Supper Co.) containing the NR solutions were sealed and mounted at a distance of 54 cm from the detector and perpendicular to the beam direction. Datasqueeze Software (www.datasqueezesoftware.com) was used for data analysis.

Received: January 13, 2008
Published online: May 26, 2008

[1] G. M. Whitesides, B. Grzybowski, *Science* **2002**, *295*, 2418.
[2] G. M. Whitesides, M. Boncheva, *Proc. Natl. Acad. Sci. USA* **2002**, *99*, 4769.
[3] A. P. Alivisatos, *Science* **1996**, *271*, 933.
[4] X. G. Peng, L. Manna, W. D. Yang, J. Wickham, E. Scher, A. Kadavanich, A. P. Alivisatos, *Nature* **2000**, *404*, 59.
[5] V. L. Colvin, M. C. Schlamp, A. P. Alivisatos, *Nature* **1994**, *370*, 354.
[6] M. D. Fischbein, M. Drndić, *Appl. Phys. Lett.* **2005**, *86*, 193106.
[7] See, for example, N. C. Greenham, X. G. Peng, A. P. Alivisatos, *Phys. Rev. B* **1996**, *54*, 17628.
[8] See, for example, M. Bruchez, M. Moronne, P. Gin, S. Weiss, A. P. Alivisatos, *Science* **1998**, *281*, 2013.
[9] X. M. Lin, H. M. Jaeger, C. M. Sorensen, K. J. Klabunde, *J. Phys. Chem. B.* **2001**, *105*, 3353.
[10] C. B. Murray, C. R. Kagan, M. G. Bawendi, *Science* **1995**, *270*, 1335.
[11] E. V. Shevchenko, D. V. Talapin, N. A. Kotov, S. O'Brien, C. B. Murray, *Nature* **2006**, *439*, 55.
[12] L.-S. Li, J. Walda, L. Manna, A. P. Alivisatos, *Nano Lett.* **2002**, *2*, 557.
[13] S. D. Bunge, K. M. Krueger, T. J. Boyle, M. A. Rodriguez, T. J. Headley, V. L. Colvin, *J. Mater. Chem.* **2003**, *13*, 1705.
[14] D. V. Talapin, E. V. Shevchenko, C. B. Murray, A. Kornowski, S. Förster, H. Weller, *J. Am. Chem. Soc.* **2004**, *126*, 12984.
[15] L. Carbone, C. Nobile, M. De Giorgi, F. Della Sala, G. Morello, P. Pompa, M. Hytch, E. Snoeck, A. Fiore, I. R. Franchini, M. Nadasan, A. F. Silvestre, L. Chiodo, S. Kudera, R. Cingolani, R. Krahne, L. Manna, *Nano Lett.* **2007**, *7*, 2942.
[16] D. V. Talapin, J. H. Nelson, E. V. Shevchenko, S. Aloni, B. Sadtler, A. P. Alivisatos, *Nano Lett.* **2007**, *7*, 2951.
[17] A. Ghezelbash, B. Koo, B. A. Korgel, *Nano Lett.* **2006**, *6*, 1832.
[18] M. Li, H. Schnablegger, S. Mann, *Nature* **1999**, *402*, 393.
[19] B. Nikoobakht, Z. L. Wang, M. A. El-Sayed, *J. Phys. Chem. B* **2000**, *104*, 8635.
[20] N. R. Jana, L. A. Gearheart, S. O. Obare, C. J. Johnson, K. J. Edler, S. Mann, C. J. Murphy, *J. Mater. Chem.* **2002**, *12*, 2909.
[21] P. Yang, F. Kim, *ChemPhysChem* **2002**, *3*, 503.
[22] S. Ahmed, K. M. Ryan, *Nano Lett.* **2007**, *7*, 2480.
[23] K. M. Ryan, A. Mastroianni, K. A. Stancil, H. Liu, A. P. Alivisatos, *Nano Lett.* **2006**, *6*, 1479.
[24] Z. Hu, M. D. Fischbein, C. Querner, M. Drndić, *Nano Lett.* **2006**, *6*, 2585.
[25] R. D. Deegan, O. Bakajin, T. F. Dupont, G. Huber, S. R. Nagel, T. A. Witten, *Nature* **1997**, *389*, 827.
[26] R. D. Deegan, O. Bakajin, T. F. Dupont, G. Huber, S. R. Nagel, T. A. Witten, *Phys. Rev. E* **2000**, *62*, 756.
[27] R. D. Deegan, *Phys. Rev. E* **2000**, *61*, 475.
[28] L. Shmuylovich, A. Q. Shen, H. A. Stone, *Langmuir* **2002**, *18*, 3441.
[29] E. Adachi, A. S. Dimitrov, K. Nagayama, *Langmuir* **1995**, *11*, 1057.
[30] A. P. Sommer, M. Ben-Moshe, S. Magdassi, *J. Phys. Chem. B* **2004**, *108*, 8.
[31] H. Maeda, Y. Maeda, *Langmuir* **1996**, *12*, 1446.
[32] S. Magdassi, M. Grouchko, D. Toker, A. Kamyshny, I. Balberg, O. Millo, *Langmuir* **2005**, *21*, 10264.
[33] Q. W. Li, Y. T. Zhu, I. A. Kinloch, A. H. Windle, *J. Phys. Chem. B* **2006**, *110*, 13926.
[34] R. Sharma, C. Y. Lee, J. H. Choi, K. Chen, M. S. Strano, *Nano Lett.* **2007**, *7*, 2693.
[35] M. Kimura, M. J. Misner, T. Xu, S. H. Kim, T. P. Russell, *Langmuir* **2003**, *19*, 9910.
[36] I. I. Smalyukh, O. V. Zribi, J. C. Butler, O. D. Lavrentovich, G. C. L. Wong, *Phys. Rev. Lett.* **2006**, *96*, 177801.
[37] A. P. Sommer, R. P. Franke, *Nano Lett.* **2003**, *3*, 573.
[38] J. Xu, J. F. Xia, Z. Q. Lin, *Angew. Chem. Int. Ed.* **2007**, *46*, 1860.
[39] Z. A. Peng, X. G. Peng, *J. Am. Chem. Soc.* **2001**, *123*, 1389.
[40] A. M. Alsayed, Z. Dogic, A. G. Yodh, *Phys. Rev. Lett.* **2004**, *93*, 057801.
[41] E. Rabani, D. R. Reichman, P. L. Geissler, L. E. Brus, *Nature* **2003**, *426*, 271.
[42] D. Frenkel, H. N. W. Lekkerkerker, A. Stroobants, *Nature* **1988**, *332*, 822.
[43] M. A. Bates, D. Frenkel, *J. Chem. Phys.* **2000**, *112*, 10034.
[44] P. Bolhuis, D. Frenkel, *J. Chem. Phys.* **1997**, *106*, 666.
[45] L.-S. Li, M. Marjanska, G. H. J. Park, A. Pines, A. P. Alivisatos, *J. Chem. Phys.* **2004**, *120*, 1149.
[46] L. S. Li, A. P. Alivisatos, *Phys. Rev. Lett.* **2003**, *90*, 097402.
[47] S. C. McGrother, A. Gil-Villegas, G. Jackson, *Mol. Phys.* **1998**, *95*, 657.

